



**HAL**  
open science

## Linear Camera Velocities and Point Feature Depth Estimation Using Unknown Input Observer

Rayane Benyoucef, Lamri Nehaoua, Hicham Hadj-Abdelkader, Hichem Arioui

► **To cite this version:**

Rayane Benyoucef, Lamri Nehaoua, Hicham Hadj-Abdelkader, Hichem Arioui. Linear Camera Velocities and Point Feature Depth Estimation Using Unknown Input Observer. 11th IROS Workshop on Planning, Perception, Navigation for Intelligent part of Vehicle IEEE/RSJ International Conference on Intelligent Robots and Systems (IROS 2019), Nov 2019, Macau, China. hal-02417634

**HAL Id: hal-02417634**

**<https://hal.science/hal-02417634v1>**

Submitted on 18 Dec 2019

**HAL** is a multi-disciplinary open access archive for the deposit and dissemination of scientific research documents, whether they are published or not. The documents may come from teaching and research institutions in France or abroad, or from public or private research centers.

L'archive ouverte pluridisciplinaire **HAL**, est destinée au dépôt et à la diffusion de documents scientifiques de niveau recherche, publiés ou non, émanant des établissements d'enseignement et de recherche français ou étrangers, des laboratoires publics ou privés.

# Linear Camera Velocities and Point Feature Depth Estimation Using Unknown Input Observer

R. Benyoucef, L. Nehaoua, H. Hadj-Abdelkader and H. Arioui

**Abstract**—In this paper, we propose a new approach to estimate the missing 3D information of a point feature during the camera motion and reconstruct the linear velocity of the camera. This approach is intended to solve the problem of relative localization and compute the distance between two Unmanned Aerial Vehicles (UAV) within a formation. An Unknown Input Observer is designed for the considered system described by a quasi-linear parameter varying (qLPV) model with unmeasurable variables to achieve kinematic from motion estimation. An observability analysis is performed to ensure the possibility of reconstructing the state variables. Sufficient conditions to design the observer are derived in terms of Linear Matrix Inequalities (LMIs) based on Lyapunov theory. Simulation results are discussed to validate the proposed approach.

**Keywords:** Nonlinear Observers, qLPV Systems, Feature Depth Estimation, LMI constraints, Lyapunov Theory, Kinematic from Motion.

## I. INTRODUCTION

Many works have been conducted to solve the localization problem when a team of robots cooperate with each other to achieve some defined tasks. For example in [17], this problem is solved for two terrestrial robots using exteroceptive sensors. Also In [18], a visual localization modules is proposed to estimate the relative positions of agents within a fleet of Unmanned Aerial Vehicles (UAVs).

The challenging problem of 3D structure estimation using the visual information has attracted more interest recently, we can find in literature various techniques to tackle this problem which can refer to Simultaneous Localization And Mapping (SLAM) in robotics [1] and Structure from Motion (SfM) in computer vision [2] [19].

In earlier work, researchers have addressed this problem using Stereo Vision Algorithms [3], which consists on reconstructing the depth of a feature point from two images of the same scene using triangulation. But later on, the idea of using a single camera lead to multiple other approaches, one can cite [4], where the observation of the point feature depth is achieved using the persistency of excitation lemma that results from the adaptive control theory [5], [6] and [7]. One of the major disadvantage of all these cited works is the fact that their analysis is based on the assumption of neglecting a disturbance term which affects the dynamic behavior of the system. Furthermore solutions based on Extended Kalman Filter (EKF) have been proposed in [8] [9]. However the main drawback of this approach is that they involve a certain

degree of linearization which contradicts most of the studied system dynamics. In the present paper, we achieve the estimation of the 3D information of a feature point together with recovering the linear velocity of the camera with respect to  $x$  and  $y$  axis assuming a perfect knowledge of the angular velocity of the camera and the linear velocity with respect to its  $z$  axis. The system is described with qLPV representation [13][14] and based on the new description of the system, An unknown input observer (UIO) is designed, which allows estimating the state of the system in presence of unknown inputs.

Obtaining an accurate linear velocity have a significant effect on the control of autonomous vehicles and drones. The straight forward method to estimate the velocity is to use data fusion [10] where Global Positioning System (GPS) and Inertial Measurement Unit (IMU) are used for this purpose. But this method fails when it comes to indoor tasks or limited sensor resolution. Moreover, we can find in literature some other approaches. For example in [11], an Extended Kalman filter (EKF) is employed to estimate linear and angular velocity of an object during its free flight, on the other hand in [12], Riccati observer is used to solve this problem. This work focuses on solving the relative localization problem for coordination and control of multiple autonomous aerial agents using the data provided by the on-board cameras of the UAVs to estimate the relative distance from the other agents with respect to its camera reference frame and reconstruct the relative velocity of the camera. This information is essential for data fusion or to give an accurate estimate of the absolute velocity of the vehicle.

The main contribution of this work can be summarised in two points the first one is introducing a novel description of the relation between the variation of the feature extracted from an image and the linear/angular velocities of the camera using qLPV representation, based on which a nonlinear observer is designed to estimate the depth, and the second point consists on reconstructing the camera linear velocity with respect to its  $x$  axis and  $y$  axis during its motion.

This paper is structured as follows: in section II, basic definitions are highlighted and the nonlinear model of camera is described. In section III, the new description using qLPV representation is explained for the nonlinear model of camera. In Section IV the design of the nonlinear observer is presented and the sufficient conditions are given in terms of LMIs based on Lyapunov theory. Simulation tests are conducted to discuss the performances of the proposed observer in section V. Finally, section VI draws some conclusions regarding our work.

All authors are with IBISC Lab, Evry Val d'Essonne (UEVE), Paris Saclay University, 43 Rue du Pelvoux, 91080 Courcouronnes. France rayane.benyoucef@univ-evry.fr

## II. MATHEMATICAL BACKGROUND

In this section, we first provide some basic definitions and lemmas needed for the development of the proposed approach. Then, we recall the conventional camera model.

### A. Notations and basic definitions

We represent matrices in upper case bold letters  $\mathbf{X}$  and vectors in lower case bold letters  $\mathbf{x}$  otherwise, the remaining notations represent scalars ( $x$  or  $X$ ).

We recall in the following the theorems used in the analysis of the observer convergence:

*Theorem 1 (Strong Detectability Condition):* For every matrix  $\mathbf{A} \in \mathbb{R}^{n \times n}$ ,  $\mathbf{F} \in \mathbb{R}^{n \times q}$  and  $\mathbf{C} \in \mathbb{R}^{m \times n}$ . We consider the following Linear Time Invariant (LTI) system:

$$\begin{cases} \dot{\mathbf{x}}(t) = \mathbf{A}\mathbf{x}(t) + \mathbf{F}\mathbf{d}(t) \\ \mathbf{y}(t) = \mathbf{C}\mathbf{x}(t) \end{cases} \quad (1)$$

where  $\mathbf{x} \in \mathbb{R}^n$ ,  $\mathbf{y} \in \mathbb{R}^m$  and  $\mathbf{d} \in \mathbb{R}^q$  are respectively the state vector, the unknown input vector and the output vector. The system (1) is strongly detectable if:

$$\lim_{t \rightarrow \infty} y(t) = 0 \Rightarrow \lim_{t \rightarrow \infty} x(t) = 0 \quad (2)$$

regardless of the input and the initial state. Algebraically this is equivalent to:

$$\text{rank}(\mathbf{R}(p)) = n + q \quad (3)$$

where  $p$  represents the pole of the system and  $\mathbf{R}$  denotes the Rosenbrock matrix of system (1), given by:

$$\mathbf{R} = \begin{bmatrix} p\mathbf{I} - \mathbf{A} & -\mathbf{F} \\ \mathbf{C} & 0 \end{bmatrix} \quad (4)$$

*Lemma 1:* For every matrix  $\mathbf{G} = \mathbf{G}^T > 0$ ,  $\mathbf{X}$  and  $\mathbf{Y}$  with appropriate dimensions, the property below holds:

$$\mathbf{X}^T \mathbf{Y} + \mathbf{Y}^T \mathbf{X} \leq \mathbf{X}^T \mathbf{G} \mathbf{X} + \mathbf{Y}^T \mathbf{G}^{-1} \mathbf{Y} \quad (5)$$

*Lemma 2 (Schur complement lemma):* Consider the following convex nonlinear inequalities:

$$\mathbf{R} > 0, \quad \mathbf{T} - \mathbf{S}\mathbf{R}^{-1}\mathbf{S}^T > 0 \quad (6)$$

where the matrices  $\mathbf{T} = \mathbf{T}^T$ ,  $\mathbf{R} = \mathbf{R}^T$  and  $\mathbf{S}$  are of appropriate dimension. Hence, the previous inequalities can be written in the following form:

$$\begin{bmatrix} \mathbf{T} & \mathbf{S} \\ \mathbf{S}^T & \mathbf{R} \end{bmatrix} > 0 \quad (7)$$

Note that the previous mathematical properties for the LTI systems hold for the case of qLPV systems considering the case of frozen parameter vectors.

### B. Conventional camera model

Let  $\mathbf{p}$  be a 3-D point of coordinates  $\mathbf{p} = (X \ Y \ Z)^T$  defined in the camera frame  $\mathcal{F}_c$ . Its projection onto the image plane is obtained through the well-known Pinhole model.

More precisely, the 3-D point  $\mathbf{p}$  is projected in the image as a 2-D point with homogeneous coordinates given by the vector  $\mathbf{m}$  as:

$$\mathbf{m} = (x \ y \ 1)^T = \frac{1}{Z} \mathbf{p} \quad (8)$$

The velocity of the 3D point  $p$  is related to the camera special velocity by:

$$\dot{\mathbf{p}} = -v \mathbf{p} + \mathbf{p} \times \boldsymbol{\omega} = (-\mathbf{I} \quad [\mathbf{p}]_{\times}) \mathbf{u} \quad (9)$$

where  $[\ ]_{\times}$  refers to the skew-symmetric matrix of a given vector,  $\mathbf{u} = (v^T \ \boldsymbol{\omega}^T)^T$  is the spatial velocity of the camera motion, with  $v = (v_x \ v_y \ v_z)^T$  and  $\boldsymbol{\omega} = (\omega_x \ \omega_y \ \omega_z)^T$  are respectively, the instantaneous linear and angular velocities of the camera frame. From (9), the dynamics of the inverse of the depth  $\frac{1}{Z}$  is given by:

$$\frac{d}{dt} \left( \frac{1}{Z} \right) = \left( 0 \quad 0 \quad -\frac{1}{Z^2} \quad -\frac{y}{Z} \quad \frac{x}{Z} \quad 0 \right) \mathbf{u} \quad (10)$$

The time derivative of the image point  $\mathbf{m}$  is linked to the camera spatial velocity  $\mathbf{u}$  by the following interaction matrix [13]:

$$\dot{\mathbf{m}} = \begin{pmatrix} -\frac{1}{Z} & 0 & \frac{x}{Z} & xy & -(1+x^2) & y \\ 0 & -\frac{1}{Z} & \frac{y}{Z} & (1+y^2) & -xy & -x \end{pmatrix} \mathbf{u} \quad (11)$$

Let us now define the state vector as  $\mathbf{x} = (\mathbf{s}^T, \chi)^T$  with  $\mathbf{s} = (x \ y)^T \in \mathbb{R}^2$  is a *measurable* vector, and  $\chi = \frac{1}{Z} \in \mathbb{R}$  is the *unmeasurable* 3D data that we want to estimate. Using (11) and (10), the dynamics of the state vector  $\mathbf{x}$  is given by:

$$\begin{cases} \dot{\mathbf{s}} = \mathbf{f}_m(\mathbf{s}, \mathbf{u}) + \boldsymbol{\Omega}^T(\mathbf{s}, \mathbf{u}) \chi \\ \dot{\chi} = \mathbf{f}_u(\mathbf{s}, \chi, \mathbf{u}) \end{cases} \quad (12)$$

where the vectors  $\boldsymbol{\Omega}^T(\mathbf{s}, \mathbf{u}) \in \mathbb{R}^2$ ,  $\mathbf{f}_m(\mathbf{s}, \mathbf{u}) \in \mathbb{R}^2$  and  $\mathbf{f}_u(\mathbf{s}, \chi, \mathbf{u}) \in \mathbb{R}$  are generic and sufficiently smooth w.r.t their arguments and they are defined as:

$$\begin{cases} \mathbf{f}_m(\mathbf{s}, \mathbf{u}) = \begin{pmatrix} xy & -(1+x^2) & y \\ 1+y^2 & -xy & -x \end{pmatrix} \boldsymbol{\omega} \\ \boldsymbol{\Omega}(\mathbf{s}, \mathbf{u}) = (-v_x + x v_z \quad -v_y + y v_z) \\ \mathbf{f}_u(\mathbf{s}, \chi, \mathbf{u}) = v_z \chi^2 + (y \omega_x - x \omega_y) \chi \end{cases} \quad (13)$$

In the upcoming sections, the dynamic model given in (12) will be expressed in a qLPV form in order to design a proper nonlinear Unknown Input (UI) Observer to estimate the depth information  $\chi$  and recover the linear velocities with respect to the  $x$  and  $y$  axis of the camera.

### III. POLYTOPIC FORMULATION & DETECTABILITY ANALYSIS

We express in this section, the vision system model (13) into qLPV structure and analyze the existence of the nonlinear UI observer.

The objective of this paper is to estimate the depth information  $\frac{1}{Z}$  and reconstruct the linear velocities during the camera motion using a nonlinear unknown input observer. For this purpose, we represent the system (12) in a state space form as follows:

$$\begin{cases} \dot{\mathbf{x}} &= \mathbf{A}(\mathbf{x}, \mathbf{u}) \mathbf{x} + \mathbf{B}(\mathbf{y}) \boldsymbol{\omega} + \mathbf{F} \mathbf{d} \\ \mathbf{y} &= \mathbf{C}\mathbf{x} \end{cases} \quad (14)$$

where:

$$\mathbf{A}(\mathbf{x}, \mathbf{u}) = \begin{pmatrix} 0 & 0 & xv_z \\ 0 & 0 & yv_z \\ y\omega_x & x\omega_y & \chi v_z + \omega_x y - x\omega_y \end{pmatrix}$$

$$\mathbf{B}(\mathbf{y}) = \begin{pmatrix} xy & -(1+x^2) & y \\ 1+y^2 & -xy & -x \\ -xy & -xy & 0 \end{pmatrix}$$

$$\mathbf{F} = \begin{pmatrix} 1 & 0 \\ 0 & 1 \\ 0 & 0 \end{pmatrix} \quad \mathbf{d} = \begin{pmatrix} -\chi v_x \\ -\chi v_y \end{pmatrix}$$

and  $\mathbf{y}$  represents the output of the system with:

$$\mathbf{C} = \begin{pmatrix} 1 & 0 & 0 \\ 0 & 1 & 0 \end{pmatrix}$$

Using the sector nonlinearity approach, the previous system (14) can be represented in the polytopic form as follows:

$$\begin{cases} \dot{\mathbf{x}} &= \sum_{i=1}^r \mu_i(\mathbf{x}) (\mathbf{A}_i \mathbf{x} + \mathbf{B}(\mathbf{y}) \boldsymbol{\omega} + \mathbf{F} \mathbf{d}) \\ \mathbf{y} &= \mathbf{C}\mathbf{x} \end{cases} \quad (15)$$

where  $\mathbf{A}_i \in \mathbb{R}^{3 \times 3}$ ,  $\mathbf{B}(\mathbf{y}) \in \mathbb{R}^{3 \times 3}$  and  $\mu_i, i = 1, \dots, r$  are the weighting functions with  $r$  is the number of sub-models that depends on the number of nonlinearities in the system (in our case we have five nonlinearities). These weighting functions satisfy the following convex sum property on the considered compact bounds of the nonlinearities of the system:

$$\begin{cases} 0 \leq \mu_i \leq 1 \\ \sum_{i=1}^r \mu_i = 1 \end{cases} \quad (16)$$

Note that in hereafter we are going to consider the discrete-time form of the continuous-time system (15) represented before and keep the same notations. Using Forward Euler Approximation for state space models, the previous system will have the following form:

$$\begin{cases} \mathbf{x}(k+1) &= \sum_{i=1}^r \mu_i(\mathbf{x}(k)) (\mathbf{A}_i \mathbf{x}(k) + \mathbf{B}(\mathbf{y}(k)) \boldsymbol{\omega}(k) + \mathbf{F} \mathbf{d}(k)) \\ \mathbf{y}(k) &= \mathbf{C}\mathbf{x}(k) \end{cases} \quad (17)$$

with  $k$  is the sampling instant.

The new description of the model enables us to synthesis a proper nonlinear unknown input observer to estimate the depth information and reconstruct the linear velocities. This type of observer exists under the following conditions:

- 1)  $rank(\mathbf{C}\mathbf{F}) = rank(\mathbf{F})$ .
- 2) the system (14) is strong detectable, that means, it satisfies the condition stated in theorem (1)

After verifying the two conditions above, we can state that the UI observer exists. In the next section, we discuss the observer design.

### IV. DESIGN OF THE UI OBSERVER

In this section we present the UI Observer design given in the form:

$$\begin{cases} \mathbf{z}(k+1) &= \sum_{i=1}^r \mu_i(\hat{\mathbf{x}}(k)) (\mathbf{N}_i \mathbf{z}(k) + \mathbf{G}_i \boldsymbol{\omega}(k) + \mathbf{L}_i \mathbf{y}(k)) \\ \hat{\mathbf{x}}(k) &= \mathbf{z}(k) - \mathbf{E}\mathbf{y}(k) \end{cases} \quad (18)$$

where  $\mathbf{z} \in \mathbb{R}^3$  is the state of the observer and  $\hat{\mathbf{x}} \in \mathbb{R}^3$  the estimated state and the matrices  $\mathbf{N}_i$ ,  $\mathbf{G}_i$ ,  $\mathbf{L}_i$  and  $\mathbf{E}$  are the matrices gains to be computed such that the state estimation error given by (19) converges to zero.

$$\begin{aligned} \mathbf{e}(k) &= \mathbf{x}(k) - \hat{\mathbf{x}}(k) \\ &= (\mathbf{I} + \mathbf{E}\mathbf{C}) \hat{\mathbf{x}}(k) - \mathbf{z}(k) \end{aligned} \quad (19)$$

With  $\mathbf{T} = \mathbf{I} + \mathbf{E}\mathbf{C}$ , the error will be defined as:

$$\mathbf{e}(k) = \mathbf{T} \hat{\mathbf{x}}(k) - \mathbf{z}(k) \quad (20)$$

For sake of simplicity, in what follows we put:  $e(k) = e_k$ . Thus, the expression of the estimation error is equivalent to:

$$\begin{aligned} \mathbf{e}_{k+1} &= \mathbf{T} \hat{\mathbf{x}}_{k+1} - \mathbf{z}_{k+1} \\ &= \sum_{i=1}^r \mu_i(\hat{\mathbf{x}}_k) (\mathbf{N}_i \mathbf{e}_k + (\mathbf{T} \mathbf{A}_i - \mathbf{K}_i \mathbf{C} - \mathbf{N}_i) \mathbf{x}_k + \mathbf{T} \mathbf{F} \mathbf{d}_k + (\mathbf{T} \mathbf{B}_i - \mathbf{G}_i) \boldsymbol{\omega}_k) + \Delta \end{aligned} \quad (21)$$

with  $\Delta = \mathbf{T} (\mu_i(\mathbf{x}_k) - \mu_i(\hat{\mathbf{x}}_k)) (\mathbf{A}_i \mathbf{x}_k + \mathbf{B}_i \boldsymbol{\omega}_k + \mathbf{F} \mathbf{d}_k)$  and  $\mathbf{K}_i = \mathbf{N}_i \mathbf{F} - \mathbf{L}_i$ .

We assume that all the elements in  $\Delta$  are growth bounded with respect to  $\mathbf{e}_k$ . Thus we can say that  $\Delta$  fulfills the calmness property at the origin:

$$\Delta^T \Delta = \|(\Delta\|^2 < \alpha^2 \|\hat{\mathbf{x}}_k - \mathbf{x}_k\|^2 = \alpha^2 \|\mathbf{e}_k\|^2 \quad (22)$$

The notation  $\|\cdot\|$  represents the 2-norm and  $\alpha^2 > 0$  is constant of Lipschitz.

To ensure the stability of the error dynamics (21), the following conditions must be satisfied  $\forall i = 1, \dots, 32$ :

- 1) The system defined by:  $\mathcal{N}_i = \sum_{i=1}^r \mu_i(\hat{\mathbf{x}}_k) \mathbf{N}_i$  is stable where:  $\mathbf{e}_{k+1} = \mathcal{N}_i \mathbf{e}_k + \Delta$ .
- 2)  $\mathbf{T} \mathbf{A}_i - \mathbf{K}_i \mathbf{C} - \mathbf{N}_i = 0$
- 3)  $\mathbf{T} \mathbf{B}_i - \mathbf{G}_i = 0$
- 4)  $\mathbf{T} \mathbf{F} = 0$

The first condition implies that  $\mathcal{N}_e$  is Hurwitz subject to a vanishing disturbance  $\Delta$  i.e:  $\Delta \rightarrow 0$  when  $\hat{\mathbf{x}} \rightarrow \mathbf{x}$  and to

demonstrate that [16], we consider the following quadratic Lyapunov function:

$$V = \mathbf{e}_k^T \mathbf{P} \mathbf{e}_k \quad \mathbf{P} = \mathbf{P}^T > 0 \quad (23)$$

It follows that:

$$\begin{aligned} V_{k+1} - V_k &= \mathbf{e}_{k+1}^T \mathbf{P} \mathbf{e}_{k+1} - \mathbf{e}_k^T \mathbf{P} \mathbf{e}_k \\ &= \mathbf{e}_k^T \mathcal{N}_e^T \mathbf{P} \mathcal{N}_e \mathbf{e}_k + \Delta_k^T (\mathbf{X}, \hat{\mathbf{X}}) \mathbf{P} \mathcal{N}_e \mathbf{e}_k + \\ &\quad \mathbf{e}_k^T \mathcal{N}_e^T \mathbf{P} \Delta + \Delta^T \mathbf{P} \Delta \end{aligned} \quad (24)$$

To ensure the stability of the system the time derivative of the Lyapunov function must satisfy:

$$\mathbf{e}_k^T \mathcal{N}_e^T \mathbf{P} \mathcal{N}_e \mathbf{e}_k + \Delta_k^T (\mathbf{X}, \hat{\mathbf{X}}) \mathbf{P} \mathcal{N}_e \mathbf{e}_k + \mathbf{e}_k^T \mathcal{N}_e^T \mathbf{P} \Delta + \Delta^T \mathbf{P} \Delta < 0 \quad (25)$$

To attenuate the disturbance's effect  $\Delta$  on the estimation error  $\mathbf{e}_k$  in the  $L_2$ -gain sense, we define:

$$\sup_{\|\Delta\| \neq 0} \frac{\|\mathbf{e}_k\|}{\|\Delta\|} < \gamma^2 \quad (26)$$

which leads to the following inequality:

$$\mathbf{e}_k^T \mathbf{e}_k - \gamma^2 \Delta^T \Delta < 0 \quad (27)$$

This expression can be simplified using lemma 1, the resulting inequality is given by:

$$\Delta^T \mathbf{P} \mathcal{N}_e \mathbf{e}_k + \mathbf{e}_k^T \mathcal{N}_e^T \mathbf{P} \Delta < \epsilon \Delta^T \Delta + \frac{1}{\epsilon} \mathbf{e}_k^T \mathcal{N}_e^T \mathbf{P}^T \mathbf{P} \mathcal{N}_e \mathbf{e}_k \quad (28)$$

Then the following inequality is deduced:

$$\begin{aligned} V_{k+1} - V_k &< \mathbf{e}_k^T (\mathcal{N}_e^T \mathbf{P} \mathcal{N}_e - \mathbf{P} + \mathbf{I} + \frac{1}{\epsilon} \mathcal{N}_e^T \mathbf{P}^T \mathbf{P} \mathcal{N}_e) \mathbf{e}_k + \\ &\quad \Delta^T (\epsilon \mathbf{I} + \gamma^2 \mathbf{I} + \mathbf{P}) \Delta \end{aligned} \quad (29)$$

It follows:

$$\begin{aligned} \mathbf{e}_k^T (\mathcal{N}_e^T \mathbf{P} \mathcal{N}_e - \mathbf{P} + \mathbf{I} + \frac{1}{\epsilon} \mathcal{N}_e^T \mathbf{P}^T \mathbf{P} \mathcal{N}_e) \mathbf{e}_k + \\ \Delta^T (\epsilon \mathbf{I} - \gamma^2 \mathbf{I} + \mathbf{P}) \Delta < 0 \end{aligned} \quad (30)$$

Taken into account the Lipschitz condition (22), the following inequality holds:

$$\begin{aligned} \mathbf{e}_k^T (\mathcal{N}_e^T \mathbf{P} \mathcal{N}_e - \mathbf{P} + \mathbf{I} + \frac{1}{\epsilon} \mathcal{N}_e^T \mathbf{P}^T \mathbf{P} \mathcal{N}_e + \\ \alpha \epsilon \mathbf{I} - \alpha^2 \gamma^2 \mathbf{I} + \alpha^2 \mathbf{P}) \mathbf{e}_k < 0 \end{aligned} \quad (31)$$

The inequality (31) holds if and only if:

$$\mathcal{N}_e^T \mathbf{P} \mathcal{N}_e - \mathbf{P} + \mathbf{I} + \frac{1}{\epsilon} \mathcal{N}_e^T \mathbf{P}^T \mathbf{P} \mathcal{N}_e + \alpha^2 \epsilon \mathbf{I} - \alpha^2 \gamma^2 \mathbf{I} + \alpha^2 \mathbf{P} < 0 \quad (32)$$

Using Schur lemma 2, the inequality (32) can be expressed in an equivalent manner with the LMI constraints as:

$$\begin{bmatrix} \mathbf{I} - \mathbf{P} + \alpha^2 \epsilon \mathbf{I} - \alpha^2 \gamma^2 \mathbf{I} & \alpha \mathbf{P} & \mathcal{N}_e^T \mathbf{P} & \mathcal{N}_e^T \mathbf{P} \\ \alpha \mathbf{P} & \mathbf{P} & 0 & 0 \\ \mathbf{P} \mathcal{N}_e & 0 & -\epsilon \mathbf{I} & 0 \\ \mathbf{P} \mathcal{N}_e & 0 & 0 & -\mathbf{P} \end{bmatrix} < 0 \quad (33)$$

Substituting the term  $\mathcal{N}_e$  in the previous equation (33) yields:

$$\sum_1^r \mu_i \begin{bmatrix} \mathbf{I} - \mathbf{P} + \alpha^2 \epsilon \mathbf{I} - \alpha^2 \gamma^2 \mathbf{I} & \alpha \mathbf{P} & \mathbf{N}_i^T \mathbf{P} & \mathbf{N}_i^T \mathbf{P} \\ \alpha \mathbf{P} & \mathbf{P} & 0 & 0 \\ \mathbf{P} \mathbf{N}_i & 0 & -\epsilon \mathbf{I} & 0 \\ \mathbf{P} \mathbf{N}_i & 0 & 0 & -\mathbf{P} \end{bmatrix} < 0 \quad (34)$$

The inequality (34) is equivalent to following in more conservative manner, for all  $i = 1, \dots, 32$ :

$$\begin{bmatrix} \mathbf{I} - \mathbf{P} + \alpha^2 \epsilon \mathbf{I} - \alpha \gamma^2 \mathbf{I} & \alpha \mathbf{P} & \mathbf{N}_i^T \mathbf{P} & \mathbf{N}_i^T \mathbf{P} \\ \alpha \mathbf{P} & \mathbf{P} & 0 & 0 \\ \mathbf{P} \mathbf{N}_i & 0 & -\epsilon \mathbf{I} & 0 \\ \mathbf{P} \mathbf{N}_i & 0 & 0 & -\mathbf{P} \end{bmatrix} < 0 \quad (35)$$

From the second condition to ensure the stability of the error dynamics, one can write:  $\mathbf{N}_i = \mathbf{T} \mathbf{A}_i - \mathbf{K}_i \mathbf{C}$ . After substituting  $\mathbf{N}_i$ , We proceed to the following changing of variables:  $\bar{\lambda} = \alpha^2 \gamma^2$ ,  $\bar{\eta} = \alpha^2 \epsilon$ ,  $\mathbf{Q} = \alpha \mathbf{P}$  and  $\mathbf{W}_i = \mathbf{P} \mathbf{K}_i$  the inequality (35) becomes:

$$\begin{bmatrix} \mathbf{I} - \mathbf{P} + \bar{\eta} \mathbf{I} - \bar{\lambda} \mathbf{I} & \mathbf{Q} & \Psi^T \mathbf{P} & \Psi^T \mathbf{P} \\ \mathbf{Q} & -\mathbf{P} & 0 & 0 \\ \mathbf{P} \Psi & 0 & \epsilon \mathbf{I} & 0 \\ \mathbf{P} \Psi & 0 & 0 & -\mathbf{P} \end{bmatrix} < 0 \quad (36)$$

where  $\Psi = \mathbf{T} \mathbf{A}_i + \mathbf{W}_i \mathbf{C}$ .

Then the system (1) is stable if there exist a positive definite symmetric matrices  $\mathbf{P} \in R^{3 \times 3}$ ,  $\mathbf{Q} \in R^{3 \times 3}$ , matrices  $\mathbf{W}_i \in R^{3 \times 2}$ , positive scalars  $\bar{\eta}$  and  $\bar{\lambda}$  so that the LMIs in (36) are satisfied and the resulting observer gains are given by  $\mathbf{K}_i = \mathbf{P}^{-1} \mathbf{W}_i$

Note that in order to have feasible solution of the LMIs, the pair  $(\mathbf{T} \mathbf{A}, \mathbf{C})$  should be observable or at least detectable, we study the detectability of the system by analysing the poles. As a consequence, to fulfil the requirement of detectability the following condition must be satisfied:

$$y \omega_x + \chi v_z - x \omega_y + 1 < 0 \quad (37)$$

To summarize, after ensuring the existence of the observer, we proceed to its design according to the given steps below:

- 1) deduce  $\mathbf{E}$  from the equation (4) Since the condition  $\text{rank}(\mathbf{C} \mathbf{F}) = \text{rank}(\mathbf{F})$  holds.
- 2) calculate the matrix  $\mathbf{E}$ , the matrix  $\mathbf{T}$  is computed directly from (3) as well as the matrices  $\mathbf{G}_i$  from the equation (2).
- 3) ensure that the pair  $(\mathbf{T} \mathbf{A}, \mathbf{C})$  is at least detectable and solve the LMIs constraints (35) to get the gains  $\mathbf{K}_i = \mathbf{P}^{-1} \mathbf{W}_i$ .
- 4) Finally, compute the gain matrices:  $\mathbf{N}_i = \mathbf{T} \mathbf{A}_i - \mathbf{K}_i \mathbf{C}$  and  $\mathbf{L}_i = \mathbf{K}_i - \mathbf{N}_i \mathbf{E}$ .

The linear velocities in the  $x$  and  $y$  directions of the camera are expressed in the disturbance part of the system and they can be recovered once the estimated states converge to the real ones.

$$\mathbf{y}_{k+1} = \mathbf{C} \sum_{i=1}^r \mu_i (\mathbf{X}_k) (\mathbf{A}_i \mathbf{X}_k + \mathbf{B}(\mathbf{y}_k) \omega_k + \mathbf{F} \mathbf{d}_k) \quad (38)$$

It follows that:

$$\hat{\mathbf{d}}_k = (\mathbf{C}\mathbf{F})^{-1} \left[ \mathbf{y}_{k+1} - \mathbf{C} \sum_{i=1}^r \mu_i(\hat{\mathbf{x}}_k) (\mathbf{A}_i \hat{\mathbf{x}}_k + \mathbf{B}(\mathbf{y}_k) \omega_k) \right] \quad (39)$$

The unknown input has the given form:

$$\mathbf{d}_k = \begin{pmatrix} -\chi v_x \\ -\chi v_y \end{pmatrix} \quad (40)$$

The estimate of linear velocity with respect to  $x$  and  $y$  axis of the camera is obtained as follows:

$$\begin{pmatrix} \hat{v}_x \\ \hat{v}_y \end{pmatrix} = -\hat{\mathbf{d}}_k \hat{\chi}^{-1} \quad (41)$$

## V. SIMULATION RESULTS

In order to validate the proposed approach, we consider two sets of synthetic images generated at a rate of  $20fps$  using a known camera motion. The real depth information  $\chi$  of the tracked point feature as well as the linear velocities  $v_x$  and  $v_y$  are compared with the estimated ones and used in the discussion of the observer performance.

The LMIs conditions derived previously are solved and yield the following result:

$$\epsilon = 2.7666, \quad \bar{\lambda} = 4.5048, \quad \bar{\eta} = 1.6908$$

$$\mathbf{P} = \begin{pmatrix} 2.1209 & 0 & 0 \\ 0 & 2.1209 & 0 \\ 0 & 0 & 1.1217 \end{pmatrix}$$

$$\mathbf{Q} = 10^{-11} \begin{pmatrix} 0.0093 & 0.1220 & -0.0001 \\ 0.1220 & 0.0296 & -0.0035 \\ -0.0001 & -0.0035 & 0 \end{pmatrix}$$

The first set where original and final images are shown in figure (1), is generated using the following linear/angular velocities of the camera:

$$\begin{aligned} v_x &= 0.2 \sin(\pi t) & v_y &= -0.2 + 0.1t & v_z &= -0.7 \\ \omega_x &= 0.1 & \omega_y &= -0.2 & \omega_z &= 0 \end{aligned}$$

The red dot in the images represents the tracked point that we want to estimate its depth.



Fig. 1: (a) the original and (b) the final images of the first set of images.

To better verify the performance of the observer, we consider now a second set of images where the original and final

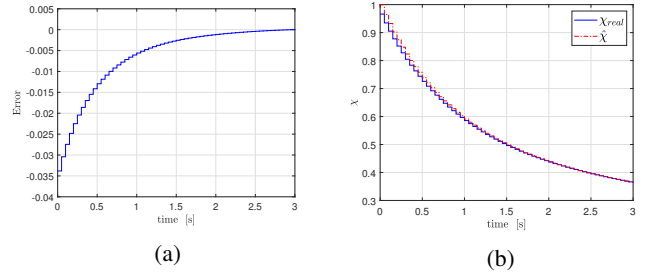


Fig. 2: (a) Estimation error (b) Real and estimated depths of the selected image point.

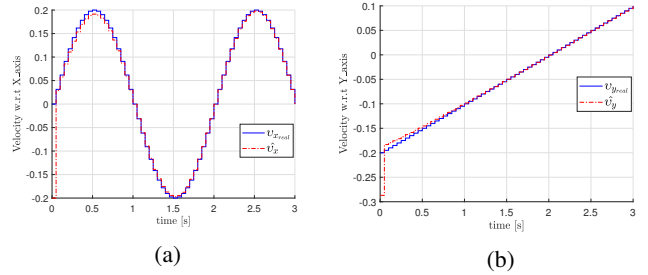


Fig. 3: Real and estimated linear velocities: (a)  $v_x$  and (b)  $v_y$ .

images are shown in figure (4). The set of images is generated using the linear/angular velocities of the camera defined below:

$$\begin{aligned} v_x &= 0.4 \cos(2\pi t) & v_y &= 0.5 \cos(\pi t) & v_z &= -0.7 \cos(\pi t) - 0.3 \\ \omega_x &= 0.1 & \omega_y &= -0.1 & \omega_z &= 0.1 \end{aligned}$$



Fig. 4: (a) the original and (b) the final images of the second set of images.

Note that the initial value of the estimated depth information  $\hat{\chi}$  is restricted by the Lipschitz condition (22). Therefore, a close initial value to the real value of the depth is required for the estimation as shown in figures (2b) and (5b).

It can be noticed from the evolution of the estimation error for the first and the second set depicted in figures (2a) and (5a) respectively, that the convergence is achieved within approximately  $2.5 \text{ sec}$ .

Figures (3) and (6) highlight the reconstructed velocities along the  $x$  and  $y$  axis respectively for both sets. From the depicted figures one can see that the velocities are



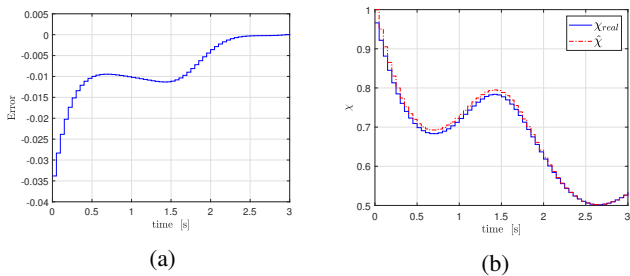


Fig. 5: (a) Estimation error (b) Real and estimated depths of the selected image point.

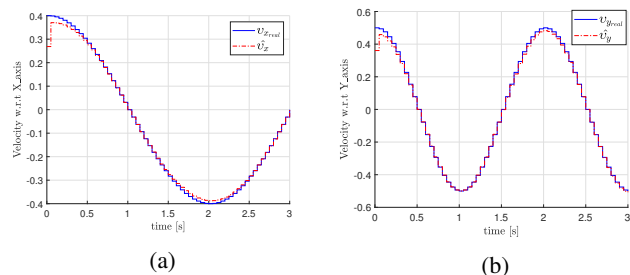


Fig. 6: Real and estimated linear velocities: (a)  $v_x$  and (b)  $v_y$ .

well recovered when the the estimated depth information  $\hat{\chi}$  converges to the real value.

Note that, to correctly estimate the depth, the velocity should be perfectly known however, In real experiments, there are very few use cases where a perfect knowledge is available, so it is required to have velocities measurements close to accurate using different techniques of filtering or data fusion for the approach to work. Usually standard triangulation techniques used in computer vision don't require strong assumptions to recover the 3d structure but with the proposed approach the linear velocity of the camera along the  $x$  and  $y$  axis can be reconstructed while estimating the depth.

## VI. CONCLUSIONS

In the present paper, we have proposed a solution to estimate the depth information of a feature point and to recover the linear velocities of the camera with respect to  $x$  and  $y$  axis. The nonlinear system describing the relationship between the feature point time variation and the camera spatial velocity has been represented by a discrete time Takagi-sugeno model. An adequate Unknown Input Observer has been designed to estimate the depth information and reconstruct the camera velocities. The convergence of the state estimation error has been analysed using the Lyapunov theory and the convergence conditions have been formulated as LMIs constraints. The performances of the proposed observer have been validated using two sets of synthetic images. Simulation results have shown the good convergence of the observer.

In future works, the proposed technique will be used to compute the relative distance between the considered UAV and the other flying robots with respect to its camera reference frame in a group formation, as well as to reconstruct the linear velocities of the UAV.

## REFERENCES

- [1] Egodagamage, R., & Tuceryan, M. (2017). Distributed monocular SLAM for indoor map building. *Journal of Sensors*, 2017.
- [2] Spica, R., & Giordano, P. R. (2013, December). A framework for active estimation: Application to structure from motion. In *52nd IEEE conference on decision and control* (pp. 7647-7653). IEEE.
- [3] Nalpantidis, L., & Gasteratos, A. (2012). Stereo vision depth estimation methods for robotic applications. In *Depth Map and 3D Imaging Applications: Algorithms and Technologies* (pp. 397-417). IGI global.
- [4] De Luca, A., Oriolo, G., & Robuffo Giordano, P. (2008). Feature depth observation for image-based visual servoing: Theory and experiments. *The International Journal of Robotics Research*, 27(10), 1093-1116.
- [5] Marino, R., & Tomei, P. (1995). *Nonlinear control design: geometric, adaptive and robust* (Vol. 136). London: Prentice Hall.
- [6] Spica, R., & Giordano, P. R. (2013, December). A framework for active estimation: Application to structure from motion. In *52nd IEEE conference on decision and control* (pp. 7647-7653). IEEE.
- [7] Spica, R., Giordano, P. R., & Chaumette, F. (2014). Active structure from motion: Application to point, sphere, and cylinder. *IEEE Transactions on Robotics*, 30(6), 1499-1513.
- [8] Guerreiro, B. J., Batista, P., Silvestre, C., & Oliveira, P. (2013). Globally asymptotically stable sensor-based simultaneous localization and mapping. *IEEE Transactions on Robotics*, 29(6), 1380-1395.
- [9] Omari, S., & Ducard, G. (2013, July). Metric visual-inertial navigation system using single optical flow feature. In *2013 European Control Conference (ECC)* (pp. 1310-1316). IEEE.
- [10] Skog, I. (2007). *GNSS-aided INS for land vehicle positioning and navigation* (Doctoral dissertation, KTH).
- [11] Jia, Y. (2017). *Estimating the Linear and Angular Velocities of a Free-Flying Object*.
- [12] Hua, M. D., & Allibert, G. (2018, August). Riccati Observer Design for Pose, Linear Velocity and Gravity Direction Estimation using Landmark Position and IMU Measurements. In *2018 IEEE Conference on Control Technology and Applications (CCTA)* (pp. 1313-1318). IEEE.
- [13] Blanchini, F., & Miani, S. (2003). Stabilization of LPV systems: state feedback, state estimation, and duality. *SIAM journal on control and optimization*, 42(1), 76-97.
- [14] Chesi, G., Garulli, A., Tesi, A., & Vicino, A. (2009). *Homogeneous polynomial forms for robustness analysis of uncertain systems* (Vol. 390). Springer Science & Business Media.
- [15] Rosinová, D., & Valach, P. (2014, May). Switched system robust control: Pole-placement LMI based approach. In *Proceedings of the 2014 15th International Carpathian Control Conference (ICCC)* (pp. 491-496). IEEE.
- [16] Bergsten, P., & Palm, R. (2000). Thau-Luenberger observers for TS fuzzy systems. In *Ninth IEEE International Conference on Fuzzy Systems*. FUZZ- IEEE, 2, pp. 671-676.
- [17] Martinelli, A., & Siegwart, R. (2005, August). Observability analysis for mobile robot localization. In *2005 IEEE/RSJ International Conference on Intelligent Robots and Systems* (pp. 1471-1476). IEEE.
- [18] Saska, M. (2015, June). MAV-swarms: unmanned aerial vehicles stabilized along a given path using onboard relative localization. In *2015 International Conference on Unmanned Aircraft Systems (ICUAS)* (pp. 894-903). IEEE.
- [19] Benyoucef, R., Nehaoua, L., Hadj-Abdelkader, H., & Arioui, H. (2019, December). Depth Estimation for a Point Feature: Structure from motion. In *IEEE CONFERENCE ON DECISION AND CONTROL* (To appear). IEEE; 2019.